

P. Anninos · I. Papadopoulos · A. Kotini
A. Adamopoulos

Differential diagnosis of prostate lesions with the use of biomagnetic measurements and non-linear analysis

Received: 1 June 2001 / Accepted: 18 December 2002 / Published online: 18 February 2003
© Springer-Verlag 2003

Abstract The purpose of this study was to investigate the biomagnetic activity emitted from the prostate gland and to differentiate cancerous from benign prostate lesions with the use of biomagnetic measurement and non-linear analysis. Magnetic recordings were obtained from 47 patients with palpable prostate lesions. Histology revealed 24 prostate cancer patients and 23 benign prostate hyperplasia (BPH) patients. The superconducting quantum interference device (SQUID) biomagnetometer was used to measure the prostate's magnetic field by placing the SQUID detector 3 mm above the symphysis pubis. The magnetic field recorded in the 2–7 Hz frequency range was of high amplitude in most malignant lesions whereas all benign cases were of low amplitude. According to our results, the sensitivity, specificity, positive predictive value and negative predictive value were 83.33%, 100%, 100% and 85.18%, respectively. By applying the Grassberger–Procaccia algorithm to the magnetoprostatogram time series in malignant and benign prostate lesions we found clear saturation in malignant prostate lesions with $m > 7$ whereas in the benign lesions there was not clear saturation. Prostate cancer emits higher biomagnetic activity than the BPH. This confirms a higher angiogenic activity in prostate cancer than the BPH lesions. Furthermore, the saturation value in the estimation of the correlation dimension of the attractor for the cancer lesions confirms the lower complexity of the system in comparison to the BPH, which is characterized by higher complexity.

Keywords Prostate cancer · Biomagnetic activity · Non-linear analysis

Introduction

Prostate cancer is a major health problem in the male population over the age of 50 due to its frequency and malignancy. It is the second leading cause of cancer-related deaths [7].

Prostate cancer mortality rates have not changed over the past 60 years despite significant advances in screening methods. It is therefore tempting to use novel technology in order to achieve a better understanding of prostate gland oncology. Patients diagnosed with prostate cancer are quite likely to discover that even leading experts disagree on the line of action which should be taken for their particular case. The detection of prostate cancer is generally based on digital rectal examination, transrectal ultrasonography (TRUS) findings and serum prostate-specific antigen (PSA) determination. However, the frequency of positive biopsies for prostate cancer has remained low. Although TRUS is widely used to guide needle biopsy, its clinical utility has been compromised by an unsatisfactory positive predictive value. Systematic sextant biopsy under ultrasound monitoring generally demonstrates prostate cancer in 20–30% of men with serum PSA levels of 4.1–10 ng/ml and in 50–67% with PSA levels of more than 10 ng/ml [6, 12, 14].

The prostate gland, like any other living tissue, emits spontaneous magnetic activity caused by ionic movements across the plasma membrane [16]. This activity, although exceedingly weak ($\sim 10^{-8}$ of the earth's magnetic field which is equivalent to 50 μT), can be measured by means of a superconducting quantum interference device (SQUID) [8, 16]. The SQUID is a diagnostic tool capable of measuring the exceedingly weak magnetic fields emitted by living tissues. The higher the concentration of living cells in the test area, the higher the biomagnetic fields produced and recorded from it. This technique has been used successfully for

P. Anninos (✉) · A. Kotini · A. Adamopoulos
Laboratory of Medical Physics, Medical School,
Democritus University of Thrace,
Paleo Nosokomio, Alexandroupolis 68100 Greece
E-mail: anninos@med.duth.gr
Tel.: +30-25510-25292
Fax: +30-25510-25292

I. Papadopoulos
Department of Urology, Medical School,
Democritus University of Thrace,
Paleo Nosokomio, Alexandroupolis 68100 Greece

studying the fetal heart [13,15], and more recently, in detecting breast tumors, brain activity and the hemodynamics of the umbilical cord [1, 2, 3, 4, 5]. It is non-invasive because the SQUID is a receiver and not a transmitter.

In this paper we report the potential value of the SQUID and the use of non-linear analysis in assessing malignant and benign prostate lesions.

Patients and methods

Magnetic recordings were obtained from 47 male patients with prostate gland lesions. Of these, 24 were diagnosed to be suffering from cancer and the other 23 to have benign lesions. The exact nature of these two categories was determined histologically by pistol-type core biopsy after magnetic recordings were performed. The age of the patients with cancer ranged from 57–73 years compared with the range of 53–75 for patients with benign disease. The Hospital Ethics Committee approved this study and informed consent was obtained from all patients prior to the procedure.

The method used for recording magnetic activity has been described in detail elsewhere [1, 2, 3, 4, 5]. In brief, we used a single channel SQUID second order gradiometer (DC SQUID model 601, Biomagnetic Technologies, USA). The gradiometer operates at low liquid helium temperatures (4°K) on the basis of the Josephson effect of superconductivity [11] with a sensitivity of 95 pT/V at 1,000 Hz. Recordings were taken in an electrically shielded room with the patient lying supine on a wooden bed, free of any metallic object, so as to decrease the environmental noise and get a better S/N ratio. In all patients, eight points were selected for examination. Four points were located at the center of the area examined, above the symphysis pubis. The other four points were located at the periphery of the area. For each point, 32 recordings of 1 s duration each were taken with the SQUID detector placed 3 mm above the recording position (Fig. 1). This allows the maximum magnetic flux to pass through the coil with little deviation from the vertical. The duration is justified because the chosen time interval is enough to cancel out, on the average, all random events and to retain only the persistent ones. The sampling frequency was 256 Hz with a bandwidth between 1 and 100 Hz. Using an AD converter, the analogue signals were converted to digital ones and, after Fourier statistical analysis, the average spectral densities from the 32 records of magnetic field strength were obtained from each one of the eight points measured in the frequency range 2–7 Hz. By convention, the maximum value was used when assessing the prostate lesions. Operators were blinded to clinical findings. In order to investigate



Fig. 1 The patient and SQUID during the MPG measurements

whether there is any differentiation in the complexity underlying the dynamics which characterized the benign and malignant prostate lesions, dimensional analysis of the existing strange attractors was applied using the chaotic analysis approach.

Chaotic analysis of magnetic prostate signals

Non-linear analysis is a powerful technique for the estimation of the dimension of the strange attractor, which characterizes the magnetoprostogram (MPG) time series obtained from patients with prostate lesions. For estimation of the dimension of the strange attractor, we considered the method proposed by Grassberger and Procaccia [9, 10], which is based on the theorem of the reconstruction of the phase space introduced by Takens [17]. According to their method, the dynamics of the system under consideration can be experimentally reconstructed from the observed time series of a single observable dynamic component, in our case the MPG. Thus, for the discrete time series $B_i = B(t_i)$ ($i = 1, 2, \dots, N$) of the MPG, measured experimentally, the vector construction of V_i is given by the following equation:

$$V_i = \{B_i, B_{i+\tau}, \dots, B_{i+(m-1)\tau}\} \quad (1)$$

The reconstruction time τ is a suitable delay parameter which may be chosen arbitrary. If the dynamics of the physical system is chaotic, the evolution of the system in the phase space, once transients die out, settles on a submanifold which is a fractal set, the strange attractor. The concept of strange attractors is of a great importance in chaotic dynamics since their existence or absence is related to the behavior of the system as chaotic or deterministic. If a strange attractor exists, it can be described by a geometrical parameter, the correlation of the fractal dimension D . This parameter is related to the number of variables required to define the space of the attractor within the phase space. Accordingly, D can be estimated from an experimental time series by means of the correlation integrals $C(r, m)$ defined as:

$$C(r, m) = \lim_{n \rightarrow \infty} (n(n-1)/2)^{-1} \sum_{i=1}^{n-1} \sum_{\substack{j=1+i \\ i \neq j}}^n \Theta(r - |V_i - V_j|) \quad (2)$$

where $\Theta(u)$ is the Heaviside function defined as ($\Theta(u) = 1$ for $u > 0$ and $\Theta(u) = 0$ for $u \leq 0$), m is the embedding dimension and n is the number of vectors constructed from a time series with N samples, given by the formula $n = N - (m-1)\tau$. The correlation integral $C(r, m)$ measures the spatial correlation of the points on the attractor and it is calculated for different values of r in the range from 0 to r_{\max} , where r_{\max} is the maximum possible distance of two randomly selected points of the attractor of the selected time series. The correlation dimension D of the attracting submanifold in the reconstruction phase space is given by:

$$D = \lim_{\substack{r \rightarrow 0 \\ m \rightarrow \infty}} \partial(\text{Ln}C(r, m)) / \partial(\text{Ln}(r)) \quad (3)$$

In the case of a chaotic signal exhibiting a strange attractor, there is a saturation value, indicated as a plateau on a graph of these slopes $\partial(\text{Ln}C(r, m)) / \partial(\text{Ln}(r))$, and which remains constant, although the signal is embedded in successively higher-dimensional phase spaces. The saturation value of the slopes gives an estimation of the correlation dimension of the attractor.

Using the above method, the correlation dimension D of the selected MPG time series was estimated for the benign and malignant lesions. The purpose of this estimation was to investigate whether there is any biological differentiation in the dynamics in these two types of lesion.

In this study, we present only one case with malignant prostate cancer and one with a benign prostate lesion. All other cases had a similar behavior to these.

Results

In Fig. 2, the wave form (raw data) of a malignant prostate lesion is shown. High amplitudes and rhythmicity characterize this MPG recording. The Fourier power spectrum, estimated by applying a FFT algorithm on the MPG data of Fig. 2, is illustrated in Fig. 3. It exhibits its maximum value (800 Ft/√Hz) at 6 Hz frequency. In Figs 4 and 5, the corresponding plots to Figs 2 and 3 are presented, analyzing the MPG data obtained from a patient with a benign prostate lesion. As shown in Fig. 4, the MPG obtained in this way does not exhibit high amplitudes and rhythmicity. The resulting Fourier power spectrum estimated by applying a FFT algorithm to the MPG data of Fig. 4 is illustrated in Fig. 5. Fig. 5 is considerably different from Fig. 3, which corresponds to the MPG recorded from a patient with a malignant prostate lesion. It exhibits a maximum value of 90 Ft/√Hz in the frequency range 2–7 Hz.

The application of the Grassberger-Procaccia algorithm to the MPG in malignant and benign prostate lesions gives us the correlation integrals illustrated in Figs 6 and 7.

In Figs 8 and 9, the slopes for different values of the embedding dimension using dimensionality calculations on the MPG of the malignant and benign prostate

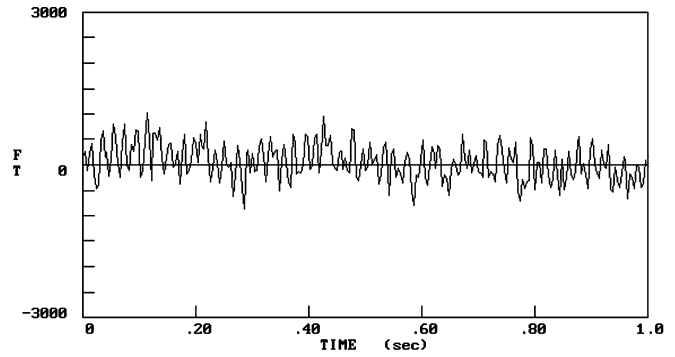


Fig. 4 The waveform of a benign prostate lesion is illustrated. It is characterized by low amplitudes and rhythmicity

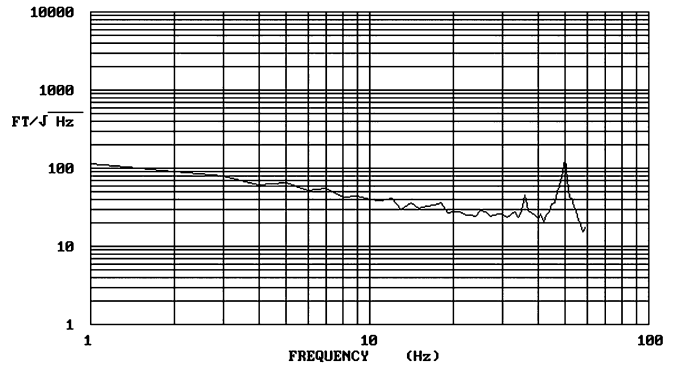


Fig. 5 The Fourier power spectrum of the raw data of Fig. 4. It exhibits a maximum value of 90 Ft/√Hz at the frequency of 2 Hz

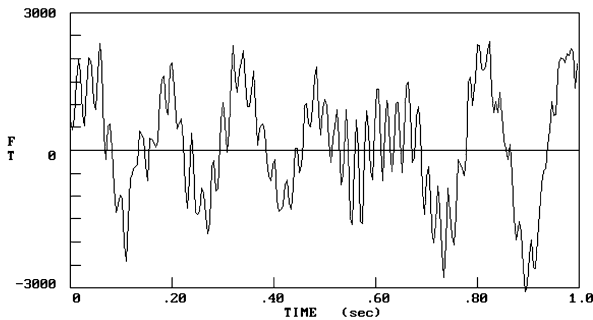


Fig. 2 The waveform of a malignant prostate lesion characterized by high amplitudes and rhythmicity

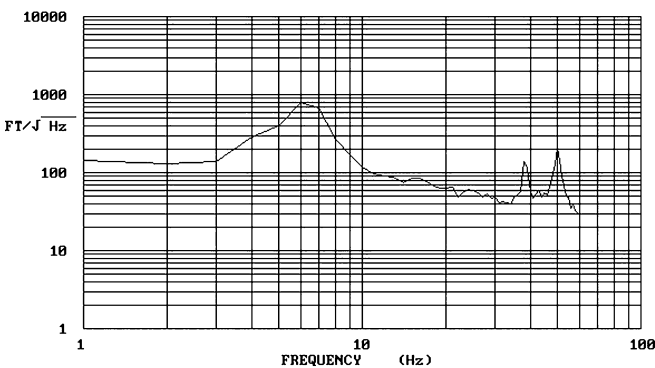


Fig. 3 The Fourier power spectrum of the raw data of Fig. 2. It exhibits a maximum value of 800 Ft/√Hz at the frequency of 6 Hz

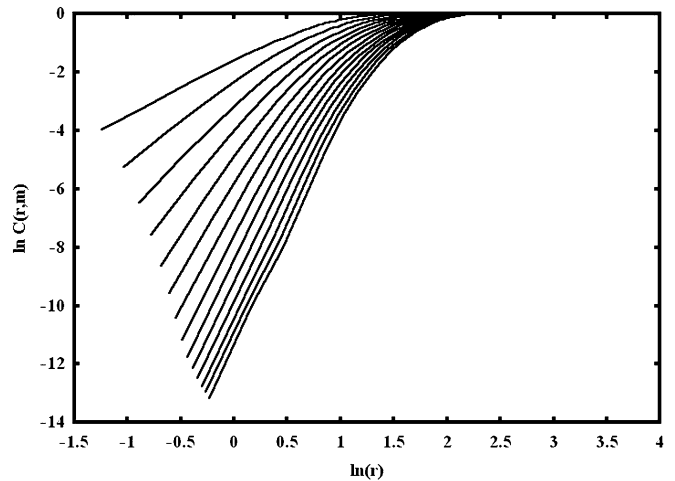


Fig. 6 The correlation integrals of the malignant MPG signal of Fig. 2

lesions are presented. Fig. 8 reveals clear saturation for $m > 7$ whereas in Fig. 9 there is no clear saturation.

Table 1 shows the relationship between biomagnetic recordings and histology in the detection of prostate cancer and hyperplasia. According to our results the sensitivity, specificity, positive predictive value and

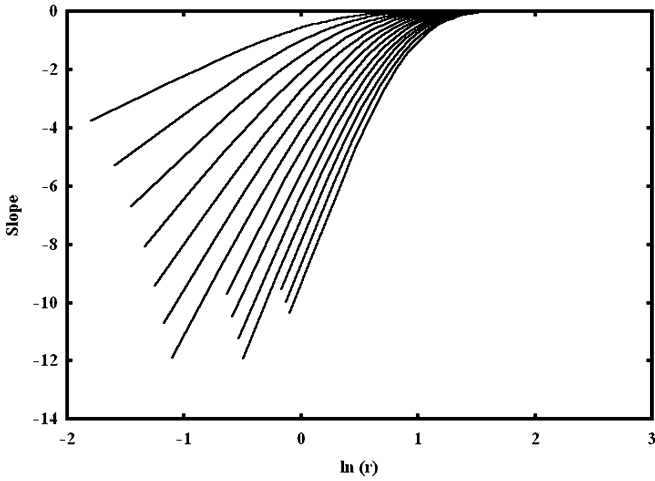


Fig. 7 The correlation integrals of the benign MPG signal of Fig. 4

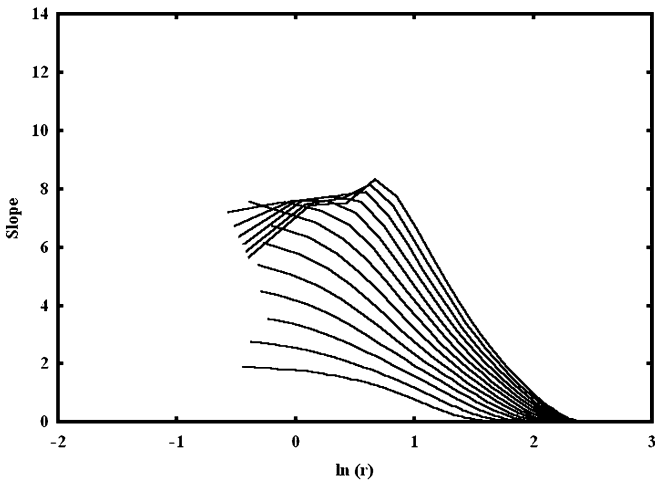


Fig. 8 The slopes of the correlation integrals of Fig. 6 which reveal clear saturation at a value > 7

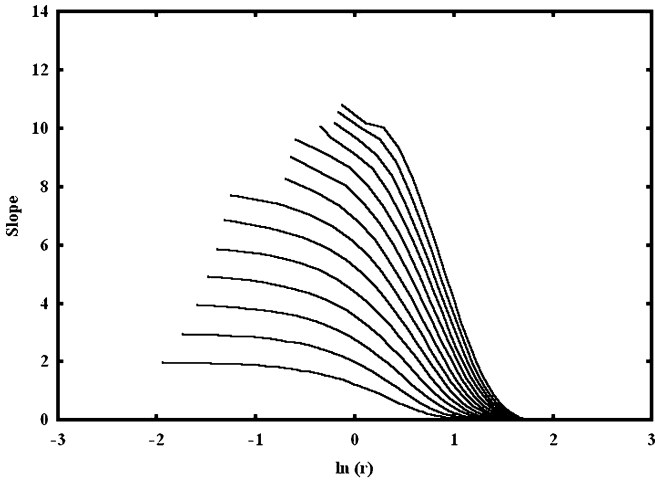


Fig. 9 The slopes of the correlation integrals of Fig 7 which reveal no saturation

Table 1 The relationship between biomagnetic recordings and histology in prostate cancer and benign prostate hyperplasia. True positive (TP)=20; true negative (TN)=23; false positive (FP)=0; false negative (FN)=4; sensitivity = $TP/(TP + FN) = 20/(20 + 4) = 83.33\%$; specificity = $TN/(TN + FP) = 23/(23 + 0) = 100\%$; positive predictive value = $TP/(TP + FP) = 20/(20 + 0) = 100\%$; negative predictive value = $TN/(TN + FN) = 23/(23 + 4) = 85.18\%$

Histology	Biomagnetic recordings	
	High amplitudes	Low amplitudes
Positive	24	20
Negative	23	0

negative predictive value were 83.33%, 100%, 100% and 85.18% respectively.

Discussion

The data presented in this study, although preliminary, justify a novel approach to MPG and suggest that this method of measuring the biomagnetic activity of prostate lesions can be potentially exploited in differentiating between benign and malignant lesions. This is not unexpected as malignant tissues, by virtue of their expansion, vascularity, and thus increased ionic movements, produce magnetic fields of higher intensity than benign hyperplastic tissues which grow more slowly.

Using non-linear analysis, it is possible to differentiate the biomagnetic activity of benign and malignant prostate lesions. Thus, the dimensionality calculations which we applied to MPG signals of malignant and benign prostate lesions were found to be useful for the evaluation of the dynamics of these systems. By comparing the correlation dimension of the strange attractors underlying the dynamics of these lesions, a saturation value around 7 (mean = 7.23, SD = 0.34) was found in the malignant lesions and an absence of saturation value in benign lesions (Figs 8, 9). Such a difference reflects an increase in the parameters which are needed in order to describe the dynamics characterizing the benign lesion. Therefore, it seems that biomagnetic measurements of prostate lesions may prove a useful method in detecting prostate carcinomas, and may offer additional information for better understanding the biology of prostate cancer.

It is true that SQUID biomagnetometry needs special equipment, a suitably prepared room and good methodological knowledge for the methods used, but once these measurements are attained the method is rewarding. It is a non-invasive procedure, reliable, rapid and easy to interpret. Furthermore, it is totally harmless and well tolerated by the subjects.

References

1. Anastasiadis P, Anninos P, Sivridis E (1994) Biomagnetic activity in breast lesions. *Breast* 3: 177

2. Anastasiadis P, Anninos P, Adamopoulos A, Sivridis E (1997) The hemodynamics of the umbilical artery in normal and pre-eclamptic pregnancies. A new application of SQUID biomagnetometry. *J Perinat Med* 25: 35
3. Anastasiadis P, Anninos P, Diamantopoulos P, Sivridis, E (1997) Fetal magnetoencephalographic mapping in normal and pre-eclamptic pregnancies *J Obstet Gynaecol* 17: 123
4. Anninos PA, Anogianakis G, Lehnertz G, Pantev CH, Hoke M (1987) Biomagnetic measurements using SQUID, *Int J Neurosci* 37: 149
5. Anninos PA, Tsagas N, Sandyk R, Derpapas K (1991) Magnetic stimulation in the treatment of partial seizures. *Int J Neurosci* 60: 141
6. Babaian RJ, Johnston DA, Naccarato W, Ayala A, Bhadkamkar VA, Fritsche HAJR (2001) The incidence of prostate cancer in a screening population with a serum prostate specific antigen between 2.5 and 4.0 ng/ml: relation to biopsy strategy. *J Urol* 165: 757
7. Crawford ED, Bennett CL, Stone NN, Knight SJ, DeAntoni E, Sharp L, Garnick MB, Porterfield HA (1997) Comparison of perspectives on prostate cancer: analyses of survey data. *Urology* 50: 366
8. Elger CE, Hoke M, Lehnertz K, Pantev C, Lutkenhoner B, Anninos PA (1989) Mapping of MEG amplitude spectra, its significance for the diagnosis of focal epilepsy. In: Maurer K (ed) *Topographic brain mapping of EEG and evoked potentials*. Springer, Heidelberg Berlin, p 567
9. Grassberger P, Procaccia I (1983) Characterization of strange attractors. *Phys Rev Lett* 50: 346
10. Grassberger P, Procaccia I (1983) Measuring the strangeness of strange attractors. *Physica D* 9: 189
11. Josephson BD (1962) Possible effects in superconducting tunneling. *Phys Lett* 1: 252
12. Karazanashvili GG, Managadze LG (2000) Model of screening of prostatic cancer among patients with prostate specific antigen concentration of 4–10 ng/ml in blood. *Urologiia* 6: 37
13. Kariniemi V, Hopelto A, Karp PJ, Katila TE (1974) The fetal magnetocardiogram. *J Perinat Med* 2: 214
14. Luboldt HJ, Bex A, Swoboda A, Husing J, Rubben H (2001) Early detection of prostate cancer in Germany: a study using digital rectal examination and 4.0 ng/ml prostate-specific antigen as cutoff. *Eur Urol* 39: 131
15. Quinn A, Weir A, Shahani U, Bain R, Maas P, Donaldson G (1994) Antenatal fetal magnetocardiography, a new method for fetal surveillance. *Br J Obstet Gynaecol* 101: 866
16. Rose DF, Smith PD, Sato S (1987) Magnetoencephalography and epilepsy research. *Science* 238: 329
17. Takens F (1981) Detecting strange attractors in the turbulence. In: Rand DA, Young LS (eds). *Lecture notes in mathematics*. Springer, Heidelberg Berlin, p 366